

The Effects of Flap Angles on the Aerodynamic Performances of a Homebuilt Aircraft Wing Model

Nasaruddin Salam, Rustan Tarakka, Jalaluddin, and Dandhy Iriansyah

Department of Mechanical Engineering, Hasanuddin University, Gowa, Indonesia

Email: nassalam.unhas@yahoo.co.id, rustan_tarakka@yahoo.com, jalaluddin_had@yahoo.com, dandhyiriansyah@gmail.com

Muhammad Ihsan

Baramuli College of Engineering, Pinrang, Indonesia

Email: m.ihsan@stt-baramuli.ac.id

Abstract—This study focused on determining the aerodynamic performances of a homebuilt aircraft wing model developed from the NACA 23012 airfoil model with a thickness to chord ratio (t/c) of 12%. The performances are indicated by the lift coefficient (C_L) and drag coefficient (C_D) which were determined using Computational Fluid Dynamics (CFD) and an experiment conducted on the subsonic wind tunnel. A freestream velocity (U) of 40 m/s was applied while the angles of attack (α) were varied at -5° , 0° , 5° , 10° , 15° , and 20° and the flap angles at -15° , 0° , 15° , 30° , and 45° . The results showed that the alteration of the flap angles increased the maximum C_L and C_D values. This was indicated by the maximum value of 2.357 and 2.2084 recorded for the C_L at 15° angle of attack and 45° flap angle for the computation analysis and experiment respectively. Meanwhile, the maximum value of C_D was 1.2563 at a 20° angle of attack and 45° flap angle for the computational analysis. The C_L/C_D ratio was found to be 1.5501 at the particular position of the airfoil while the maximum value was 9.2982 at 0° angle of attack and 15° flap angle.

Index Terms—airfoil, angle of attack, flap angle, computational fluid dynamics, lift coefficient, drag coefficient

I. INTRODUCTION

The design of wings for homebuilt aircraft using standard models requires serious effort and this has led to a series of research over the past decades. It is important to note that one of the most popular wing models out of the 1600 airfoil models designed by NACA is the NACA 23012 airfoil. Some of the recent development in this model includes the construction of movable parts on the airfoil as well as the modification of the flap. This has led to the conduct of several studies on this model and other similar ones to investigate the effect of the airfoil flap

angle and angle of attack (α) on their lift coefficients (C_L) and drag coefficients (C_D). Some of these studies include the investigation of plain flaps as well as those that focus on Gurney flaps, multiple flaps, two-parts flaps, high-lift NACA 4412 airfoil, application of a dielectric barrier discharge (DBD) plasma actuator on flaps, viscous ground-effect on NACA 4412 airfoil, as well as modifications of the flap on a specific NACA airfoil family [1]–[9].

The investigation of pressure distribution over NACA 66-015 characterized with trailing edge flaps has found that increasing stall angles could improve wing performance [1]. Another study on NACA 0012 conducted in 2D RNG $k-\epsilon$ turbulence model computation on Gurney flap has found a tendency for a distribution of static pressure on the surface of the airfoil in low angles of attack [3]. The application of Gurney flaps has also been found to increase lift and lift-to-drag ratio in various angles of attack, based on a study of NACA 0012 airfoil in 2D-CFD using stress transport turbulence (SST) $k-\omega$ model [4]. An earlier experimental study on aerodynamic performance of a two-element airfoil, with 90° trailing edge flaps found that a flap which was 5% longer than the chord, can significantly increase the lift of the baseline airfoil, over a wide range of angles of attack. It was also found increased maximum lift coefficient on the wing flaps, with decreasing the lift-to-drag ratio [5]

Flaps on wings with a small angle of attack was found to be beneficial for small flap deflections of up to 5% of the chord, where the contribution of lift augmentation could exceed the increase in drag, resulting in an increased lift-to-drag ratio [7].

Most of the results support the application of two-equation models to numerically simulate the aerodynamics of this particular family of NACA airfoils. Meanwhile, a sub-sonic conditioned wind tunnel was discovered to be most appropriate for experimental studies.

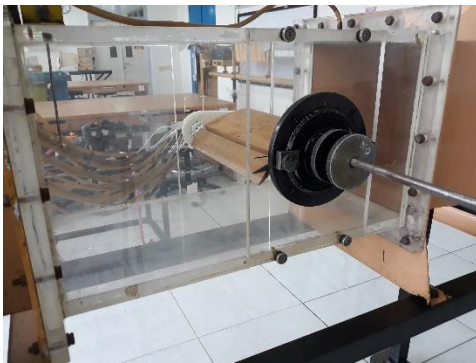
Manuscript received June 8, 2022; revised November 10, 2022.
Corresponding author : rustan_tarakka@yahoo.com

II. METHODOLOGY

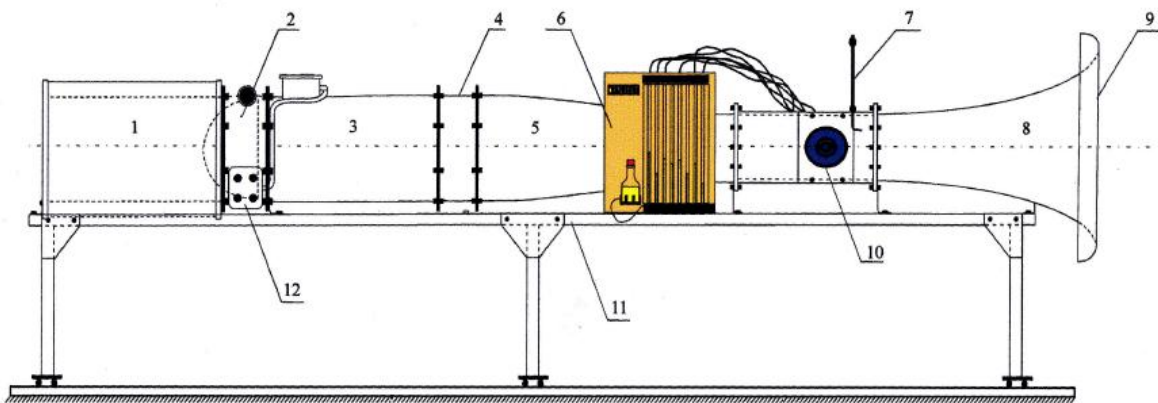
The homebuilt aircraft wing model used is a NACA 23012 airfoil model with a thickness to chord ratio (t/c) of 12%. The length of the airfoil chord is 1,600 mm while the span is 290 mm. The research was conducted using both computational and experimental approaches. The computational approach used the Computational Fluid Dynamics (CFD) program with Autodesk Fusion 360, Gambit 2.4.6, and Fluent 6.3.26 software considered suitable for NACA 23012 airfoil wing model. Meanwhile, the experimental aspect was in the form of laboratory

tests conducted on the homebuilt wing model at the subsonic wind tunnel facility in the Fluid Mechanics Laboratory, Department of Mechanical Engineering, Faculty of Engineering, Unhas Gowa.

The test model for both methods was treated with the same freestream airflow velocity (U) of 40 m/s, 6 (six) levels of the angle of attack (α) at -5° , 0° , 5° , 10° , 15° , 20° , and 5 (five) degrees of flap angle at -15° , 0° , 15° , 30° and 45° . The test model and research installation equipment are presented in Fig. 1 while the schematic diagram of the computational domain is in Fig. 2.



(a) Research test model



Remarks: 1. silencer, 2. double butterfly valve, 3. fan, 4. guide vane assembly, 5. diffuser, 6. manometer tube, 7. pitot tube, 8. effuser, 9. protection screen, 10. model holder, 11. stand level on assembly, and 12. starter.

(b) equipment setting

Figure 1. (a) Test model and (b) equipment setting.

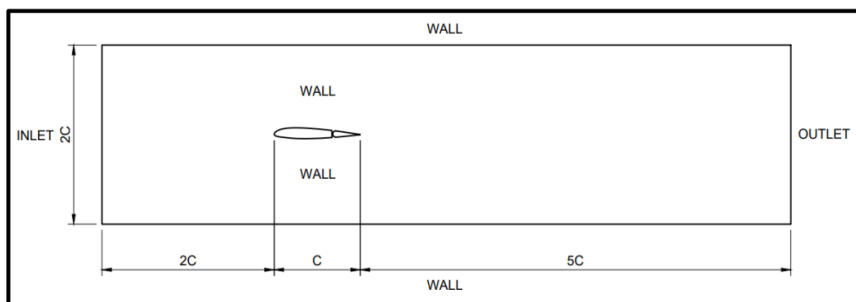


Figure 2. Schematic diagram of the computational domain.

Cengel & Cimbala defined the lift coefficient and drag coefficient using (1) and (2).

$$C_L = \frac{F_L}{\frac{1}{2} \rho U^2 A} \quad (1)$$

$$C_D = \frac{F_D}{\frac{1}{2} \rho V^2 A} \quad (2)$$

where C_L = lift coefficient, C_D = drag coefficient, ρ = mass density of air (kg/m³), U = freestream speed (m/s), A = wing platform area (m²), F_L = lifting force (N), and F_D =drag force (N) [10].

The computational approach was described using the computational domain presented in Fig. 2. Hence, the fluid flow was modeled in the k-epsilon turbulent model to represent the relationship between the turbulent kinetic energy (k) and turbulence dissipation (ϵ).

TABLE I. BOUNDARY CONDITION OF WING MODEL

Boundary condition	Types	Values (m/s)
Inlet	Velocity inlet	40
Outlet	Pressure outlet	
Model	Wall	
Wall/wind tunnel	Wall	

III. RESULTS AND DISCUSSION

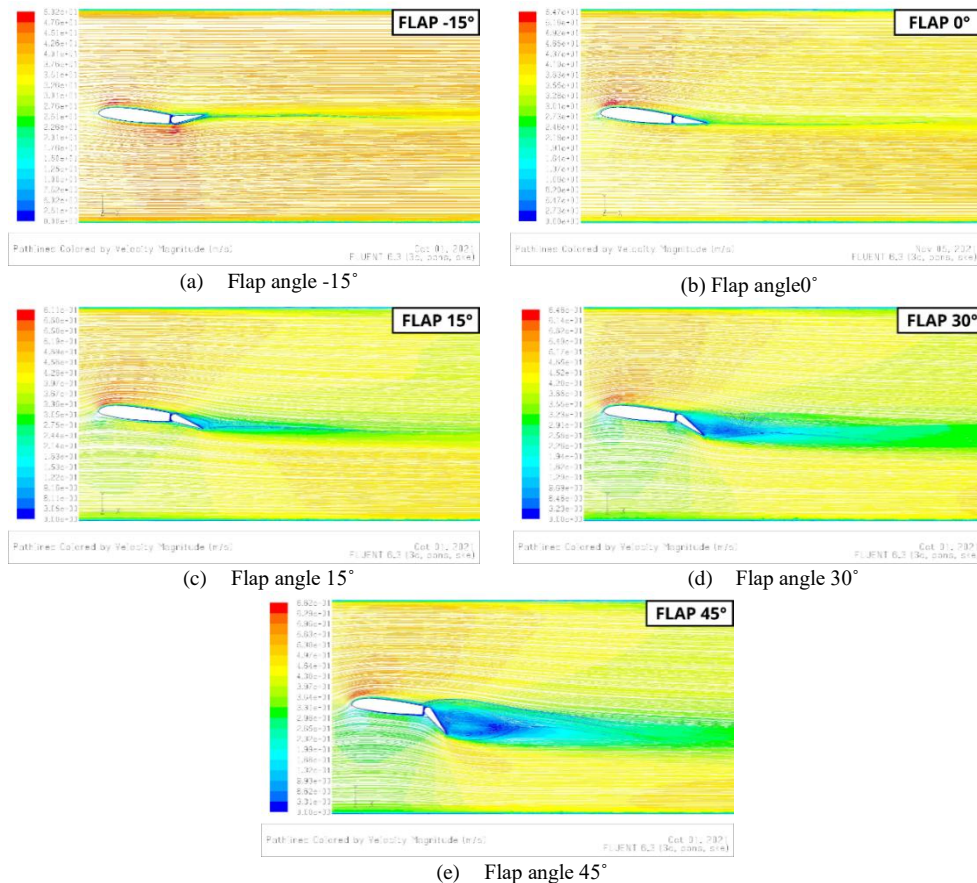


Figure 2. Flow characteristics on the airfoil with a 5° angle of attack and different variations of flap angle at a freestream speed of 40 m/s.

The flow characteristics at flap angles 15°, 30°, and 45° are presented in Fig. 2 (c,d,e) respectively and the flow was observed on the trailing edge moving from the lower surface to the upper surface to later form a vortex which became bigger at a flap angle of 45°. This is associated with the lower pressure on the upper surface compared to the lower surface, thereby, causing the flow of air through the tip of the airfoil. It is important to note that the vortex,

The results are arranged in such a framework that the flow characteristics for all flap angles are explained while the underlying analysis is also presented through general reasoning for the particular phenomena based on both the computational and experimental methods. The results from the computational process obtained in the form of C_L and C_D were supported by the flow pattern formed around the model in the form of a velocity path line. It is important to note that each variation of the angle of attack was analyzed several times to determine the best results.

The flow characteristics were analyzed at 5° and 15° angles of attack in the computational approach and the values obtained at 5° are presented in Fig. 2 through the velocity path line which indicates the pattern for the change in each flap angle. It was discovered that there is a significant difference between the velocity that passes through the midspan airfoil as the flap angle was varied at an angle of attack of 5°.

which was initially small in size, started getting larger as the freestream speed increased. This phenomenon led to an increase in the drag and lift forces on the airfoil. Fig. 3 shows the flow characteristics at an angle of attack of 15° and the flow on the trailing edge was also observed to be moving from the lower surface to the upper surface to form a vortex from the flap angle of 0° to 45°.

This is also caused by the lower pressure on the upper surface compared to the lower surface which allows the movement of fluid through the tip of the airfoil. The vortex observed to be initially smaller got bigger as the freestream velocity increased, hence the largest vortex was found at a flap angle of 45°. This phenomenon

increased the drag and lift forces on the airfoil as indicated by the increase in the vortex with every change in the flap angle. The comparison of the observation for 5° and 15° angles of attack showed that the higher angles of attack have the bigger vortex as well as larger drag and lift forces at the same flap angles.

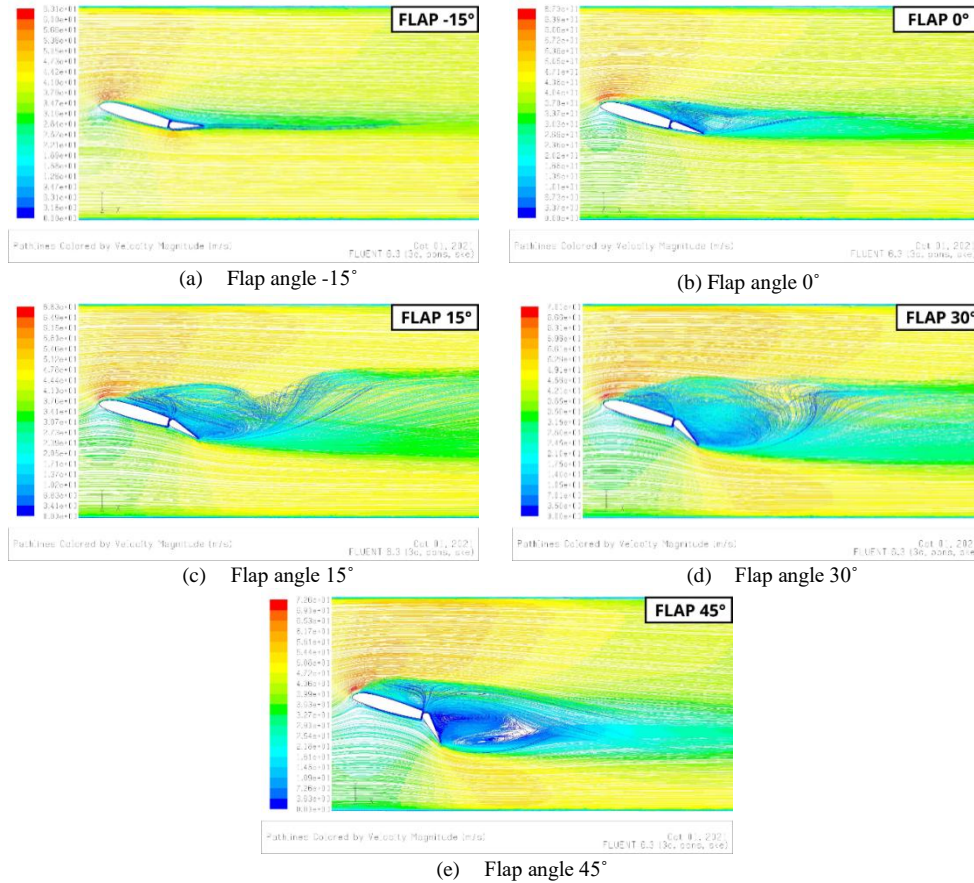


Figure 3. Flow characteristics on the airfoil with a 15° angle of attack and different variations of flap angle at a freestream speed of 40 m/s.

Table II shows the computational results of the lift coefficient (C_L) of the test model at a freestream speed of 40 m/s and an angle of attack (α) from -5° to 20° for each level of variation of flap angles. It was discovered that the lift coefficient value increased from 0° to 45° flap angles at a positive angle of attack but reduced at a negative angle of attack and flap angle. The maximum lift coefficient was found at a 15° angle of attack and 45° flap angle while the minimum was at -5° and -15° respectively. The graph of the results from the computational analysis of the lift coefficient at a constant flap angle of 5 levels is presented in Fig. 4.

TABLE II. RESULT OF COMPUTATION OF LIFT COEFFICIENT (C_L) AT FREESTREAM SPEED 40 M/S ON CHANGE OF ANGLE OF ATTACK (α) AND FLAP ANGLE

α (deg)	Flap -15°	Flap 0°	Flap 15°	Flap 30°	Flap 45°
-5	-1.0926	-0.3547	0.3636	0.8401	1.0047
0	-0.6586	0.0957	0.8733	1.2498	1.4350
5	-0.1711	0.5934	1.3344	1.6283	1.8265
10	0.2844	1.0544	1.6070	1.8982	2.1273
15	0.7417	1.3998	1.6568	1.9987	2.3547
20	0.9155	1.3654	1.4935	1.6794	1.9475

Fig. 4 shows the computational results of lift coefficients against the angles of attack at a freestream speed (U) of 40 m/s. The findings showed that the C_L value increased as the angle of attack and flap angle increased. It was also discovered that a single angle of attack was able to produce different C_L values due to the changes in the flap angle. Moreover, a greater angle of attack led to a higher C_L value and this is in line with the flow characteristics presented in Fig. 2 and Fig. 3. The findings, however, showed a stall condition for a 15° angle of attack at 0° to 45° flap angles.

Table III shows the computational results of the drag coefficients (C_D) for the test model at a freestream speed of 40 m/s and angles of attack (α) from -5° to 20° for each level of change in the flap angle. It was found that the drag coefficient value increased at the positive angle of attack and flap angle but decreased at negative angles, thereby, leading to a smaller drag coefficient. Moreover, the maximum drag coefficient was recorded at an angle of attack of 20° and a flap angle of 45° while the minimum was at 0° and 0° respectively.

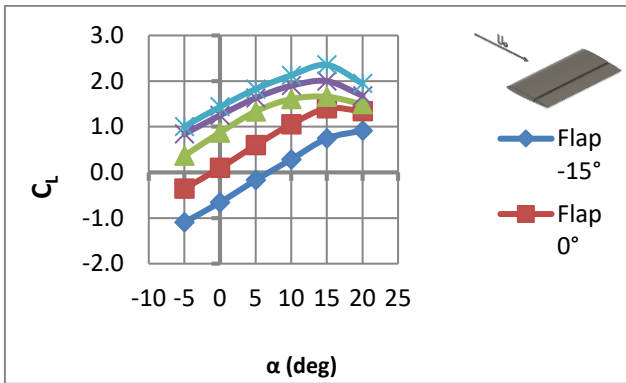


Figure 4. Flow characteristics on the airfoil with a 15° angle of attack and different variations of flap angle at a freestream speed of 40 m/s.

TABLE III. RESULTS OF COMPUTATION OF COEFFICIENT DRAG (C_D) AT FREESTREAM SPEED 40 M/S ON CHANGES IN THE ANGLE OF ATTACK (α) AND FLAP ANGLE

α (deg)	Flap -15°	Flap 0°	Flap 15°	Flap 30°	Flap 45°
-5	0.1508	0.0616	0.0663	0.1336	0.2159
0	0.0821	0.0397	0.0939	0.1781	0.2818
5	0.0569	0.0648	0.1576	0.2601	0.3911
10	0.0772	0.1327	0.2524	0.3916	0.5553
15	0.1418	0.2604	0.4184	0.6441	0.8581
20	0.2609	0.4125	0.6459	0.9582	1.2563

Fig. 5 shows the graph of the drag coefficient against the angle of attack at a freestream velocity (U) of 40 m/s and it was discovered that the value of C_D increased as the angle of attack and flap angle increased. Fig. 5 also shows that the same angle of attack has the ability to produce different C_D values due to the changes in the flap angle. It is important to note that a greater angle of attack produced a higher C_D value and this is in line with the flow characteristics presented in Fig. 2 and Fig. 3.

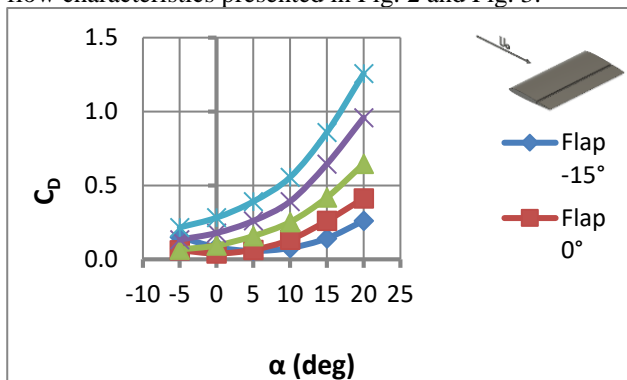


Figure 5 Graph of computed result of drag coefficient (C_D) with angle of attack (α) at freestream speed of 40 m/s and each level of change in flap Angle.

TABLE IV. THE RATIO OF THE LIFT COEFFICIENT WITH THE DRAG COEFFICIENT (C_L/C_D) AT A FREESTREAM SPEED OF 40 M/S TO CHANGES IN ANGLE OF ATTACK (α) AND FLAP ANGLE

α (deg)	Flap -15°	Flap 0°	Flap 15°	Flap 30°	Flap 45°
-5	-7.2470	-5.7571	5.4883	6.2882	4.6538
0	-8.0236	2.4146	9.2982	7.0175	5.0927
5	-3.0052	9.1535	8.4651	6.2602	4.6704
10	3.6849	7.9481	6.3675	4.8477	3.8310
15	5.2297	5.3756	3.9595	3.1031	2.7439
20	3.5083	3.2570	2.3125	1.7526	1.5501

The ratio of the lift coefficient to the drag coefficient (C_L/C_D) for the test model was determined at a freestream velocity of 40 m/s and angles of attack (α) from -5° to 20° for each level of flap angle change using computational analysis and the results are presented in Table IV. It was discovered that the C_L/C_D value decreased as the flap angles increased at 15° and 20°. The findings also showed that the minimum value at -5° to 10° angles of attack was recorded at a flap angle of -15° and the value was observed to be reduced at the flap angles of 0° to 45°. Meanwhile, the maximum, 9.2982, was found at 0° angle of attack and 15° flap angle. A similar value, 9.5135, was also recorded at a 5° angle of attack and 0° flap angle.

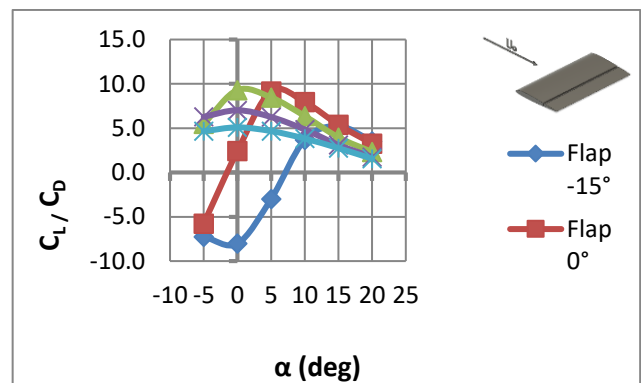


Figure 6. Graph of computational results for the ratio of lift coefficient and drag coefficient (C_L/C_D) and angle of attack (α) at a freestream speed of 40 m/s at each level of flap angle.

Fig. 6 shows the graph for the lift and drag coefficient ratio against the angle of attack at a freestream speed (U) of 40 m/s. The results showed that the C_L/C_D value increased as the angle of attack and positive flap angle were increased but a turning point was found at 0° angle of attack for 15°, 30°, and 45 flap angles. The turning point for 0° and -15° flap angle was recorded at a 15° angle of attack. It was also discovered from the Fig. 6 that a single angle of attack can produce different C_L/C_D values due to a change in the flap angle. This is the reason for the different values recorded for C_L/C_D at 0° and -15° flap angles as indicated by the large increase observed from -5° to 5° angle of attack for 0° flap angle as well as in 0° to 15° angles of attack for -15° flap angle.

TABLE V. THE RATIO OF THE LIFT COEFFICIENT TO THE DRAG COEFFICIENT (C_L/C_D) AT A FREESTREAM SPEED OF 40 M/S TO CHANGES IN ANGLE OF ATTACK (α) AND FLAP ANGLE

α (deg)	Flap -15°	Flap 0°	Flap 15°	Flap 30°	Flap 45°
-5	-1.0083	-0.3417	0.3417	0.7833	0.9833
0	-0.6167	0.0917	0.8167	1.1750	1.4167
5	-0.1583	0.5750	1.2667	1.5167	1.7417
10	0.2750	1.0083	1.5084	1.8250	2.1084
15	0.7083	1.2750	1.5584	1.9084	2.2084
20	0.8667	1.2667	1.4417	1.6584	1.8667

Table V shows the experimental results for the lift coefficient (C_L) of the test model at a freestream speed of 40 m/s and -5° to 20° angles of attack (α) for each level of change in the flap angle. It was discovered that the lift coefficient value increased from 0° to 45° flap angle in a

positive angle of attack but decrease when both the angle of attack and flap angle is negative. Moreover, the maximum lift coefficient was recorded at a 15° angle of attack and 45° flap angle while the minimum was at -5° and -15° respectively. This shows that both the computational and experimental analyses have the same trend with almost similar C_L values.

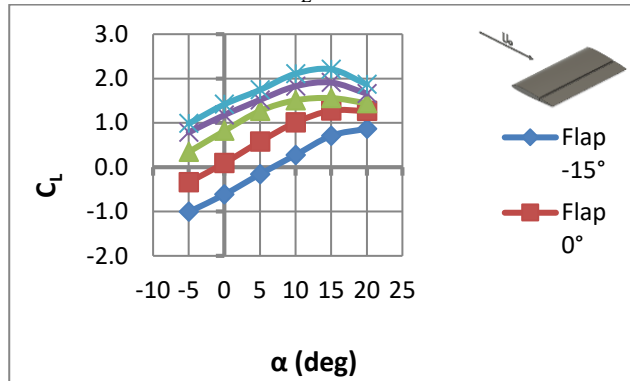


Figure 7. Graph of experimental results of the relationship between lift coefficient (C_L) and angle of attack (α) at a freestream speed of 40 m/s and each level of change in flap angle.

Fig. 7 shows a graph of the experimental results for the relationship between the lift coefficient and angle of attack at a freestream speed (U) of 40 m/s. The findings show that the C_L value increased as the angle of attack and flap angle increased. It was also indicated in Fig. 7 that a single angle of attack has the ability to produce different C_L values as long as the flap angle changes. Moreover, a greater angle of attack was observed to have led to a higher C_L value and this is in line with the flow characteristics presented in Fig. 2 and Fig. 3. However, a stall condition was observed at an angle of attack of 15° for 0° to 45° flap angles and this indicates that the findings from the computational analysis are similar to those from the experimental study.

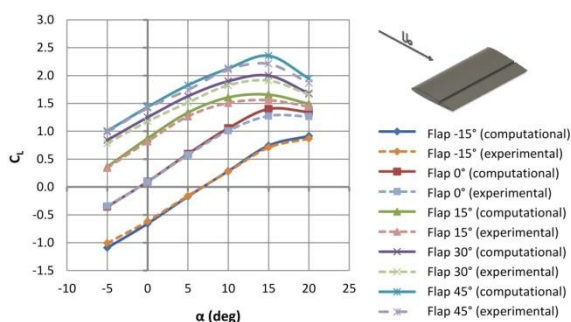


Figure 8. Comparison of computational and experimental results for the relationship between lift coefficient (C_L) and angle of attack (α) at freestream speed 40 m/s and change in each level of flap angle.

Fig. 8 shows a comparison of computational and experimental results for the relationship between lift coefficient (C_L) and angle of attack (α) at a freestream speed of 40 m/s and change in each level of flap angle. It was discovered that the C_L value is almost the same for the two analyses or with an average of 5% difference. This is also in accordance with the characteristics of the flow simulation results presented in Fig. 2 and Fig. 3.

IV. CONCLUSIONS

The fluid flow characteristics in a homebuilt aircraft wing model were analyzed using the NACA 23012 airfoil model designed with a thickness to chord ratio (t/c) of 12%. The analysis was conducted using the Computational Fluid Dynamics (CFD) program and experimentally at a freestream velocity of 40 m/s and different variations of angle of attack from -5° to 20 and flap angle from -15° to 45°. The findings showed that the lift and drag coefficients have a similar pattern at the same flap angle with different angles of attack. The maximum lift coefficient was found at a 15° angle of attack and 45° flap angle with 2.3547 recorded for the computational analysis and 2.2084 for the experiment. Moreover, the maximum drag coefficient for the computational analysis, 1.2563, was found at 20° angle of attack and 45° flap angle while the maximum C_L/C_D ratio was 9.2982 at 0° angle of attack and 15° flap angle which is almost the same as the 9.1535 recorded 5° and 0° respectively. This implies the optimal homebuilt aircraft wing model to use is the NACA 23012 airfoil model at a 15° angle of attack and 45° flap angle.

CONFLICT OF INTEREST

The authors declare no conflict of interest.

AUTHOR CONTRIBUTIONS

Dr. N. Salam, the main author, organized research promotion and conducted research planning. Dr. R. Tarakka, the corresponding author, conducted research. Dr. Jalaluddin, conducted the research, Mr. D. Iriansyah, conducted experimental research, and Mr. M. Ihsan wrote and translated the manuscript. All authors approved the final version.

ACKNOWLEDGMENTS

This research was funded by Hasanuddin University's Research and Community Service Institute, through the 2020 University Applied Research (PTU) Scheme, under the contract, No. 915/UN4.22/PT.01.03/2021, 12 April 2021. The authors express their gratitude to the head and management of the Fluid Mechanics Laboratory of the Faculty of Engineering, Hasanuddin University.

REFERENCES

- [1] I. Singh, "Effect of plain flap on the distribution over the symmetrical aerofoil NACA," *International Journal of Innovative Science and Research Technology*, vol. 2, no. 6, pp. 353–365, 2017.
- [2] S. Jain, N. Sitaram, and S. Krishnaswamy, "Computational investigations on the effects of gurney flap on airfoil aerodynamics," *International Scholarly Research Notices*, vol. 2015, p. e402358, Jan. 2015.
- [3] S. Jain, N. Sitaram, and S. Krishnaswamy, "Effect of reynolds number on aerodynamics of airfoil with gurney flap," *International Journal of Rotating Machinery*, vol. 2015, p. e628632, Sep. 2015.
- [4] M. A. Abdelrahman, W. Mohamed, I. Shahin, M. W. Al-Dosoky, and M. G. Higazy, "Aerodynamics performance of multi gurney flaps configurations on airfoil," *Engineering Research Journal*, vol. 1, no. 45, pp. 34–42, 2020.

- [5] J. Katz and R. Largman, "Effect of 90 degree flap on the aerodynamics of a two-element airfoil," *Journal of Fluids Engineering*, vol. 111, no. 1, pp. 93–94, 1989.
- [6] L. H. Feng, K. S. Choi, and J. J. Wang, "Flow control over an airfoil using virtual Gurney flaps," *Journal of Fluid Mechanics*, vol. 767, Feb. 2015.
- [7] A. E. Ockfen and K. I. Matveev, "Aerodynamic characteristics of NACA 4412 airfoil section with flap in extreme ground effect," *International Journal of Naval Architecture and Ocean Engineering*, vol. 1, no. 1, pp. 1–12, 2009.
- [8] S. K. Saha, Md. M. Alam, and A. B. M. T. Hasan, "Numerical investigation of Gurney flap aerodynamics over a NACA 2412 airfoil," in *AIP Conference Proceedings*, Jul. 2018, vol. 1980, p. 040020.
- [9] Z. Mahmood, M. K. Khan, W. J. Scale, and H. H. Bruun, "Comparison of measured and computed velocity fields over a high-lift aerofoil," *WIT Transactions on Modelling and Simulation*, vol. 12, no. 9, 1995.
- [10] Y. A. Çengel and J. M. Cimbala, *Fluid Mechanics: Fundamentals and Applications*. McGraw-Hill Education, 2018.

Copyright © 2022 by the authors. This is an open access article distributed under the Creative Commons Attribution License (CC BY-NC-ND 4.0), which permits use, distribution and reproduction in any medium, provided that the article is properly cited, the use is non-commercial and no modifications or adaptations are made.



Nasaruddin Salam – born in Bulukumba on December 20th 1959 is a Professor and the Chairman of the Fluid Mechanics Laboratory in the Department of Mechanical Engineering, Faculty of Engineering, Hasanuddin University Makassar Indonesia. He holds a doctoral degree from Brawijaya University, Malang Indonesia. His research fields include fluid dynamics, particularly on tandem bodies. Prof.

Nasaruddin Salam is a member of the Institutions of Engineers Indonesia.



Rustan Tarakka—born in Pinrang on August 27th 1975 is an Associate Professor of Mechanical Engineering, Faculty of Engineering, Hasanuddin University, Makassar, Indonesia. He holds a doctoral degree from the University of Indonesia, Jakarta, Indonesia. His research focuses on fluid dynamics and computational fluid dynamics. Dr. Tarakka is a member of the

Institutions of Engineers Indonesia.



Jalaluddin— was born in Sompu on August 25th 1972. He obtained a Doctor of Engineering in Mechanical Engineering in 2012 from Saga University Japan. He is an Associate Professor of Mechanical Engineering at Hasanuddin University, Makassar, Indonesia. His area of research covers Ground Heat Exchanger for Space Conditioning System, Renewable Energy with a focus on Solar Energy including Solar Water Heating System and Photovoltaic Applications. Dr-Eng. Jalaluddin is a member of the Institutions of Engineers Indonesia.



Dandhy Iriansyah— was born in Kadidi December 16th 1992. He graduated with a bachelor's degree from Automotive Engineering Education at the State University of Makassar. He is a postgraduate student in the Fluid Mechanics Laboratory, Department of Mechanical Engineering, Faculty of Engineering, Hasanuddin University, Makassar, Indonesia.



Muhammad Ihsan -born in Watampone, on February 20th 1977 is a lecturer at Baramuli College of Engineering, Pinrang, Indonesia. He holds dual master degrees in transport engineering from both the Asian Institute of Technology, Bangkok, Thailand, and Universitas Gajah Mada, Yogyakarta, Indonesia